Numerical Simulation of Heat Transfer During the Solidification of Pure Iron in Sand and Mullite Molds

M. M. Pariona and A. C. Mossi
Departamento de Matemática e Estatística
Programa Engenharia e Ciência de Materiais
Universidade Estadual de Ponta Grossa
Campus Uvaranas, Bloco CIPP
Laboratório Limac
84030-900 Ponta Grossa PR. Brazil
mmpariona@uepg.br

Many complex phenomena favoring the solidification of metal that occur during the casting process, such as cast metal flow, thermal gradient and heat transfer between the cast metal and the mold. The grain size and mechanical properties of cast metal are defined by both these phenomena, and by the geometrical characteristics and thermo-physical properties of the metal and the mold. Heat loss from the mold to the environment through convection can also affect the mechanical properties of cast metal. In this study reported, two-dimensional numerical simulations were made of pure iron solidification in industrial AI 50/60 AFS greensand and mullite molds, using the finite element technique and the ANSYS software program. For this purpose, the iron's thermo-physical properties were considered dependent with temperature, while for sand and mullite these properties were considered constant, and the convection phenomenon was also considered on the mold's external surface. Metallurgical characteristics, such as the attack zone in the feed head and hot top were not taken into account in this study, since they are irrelevant the behavior of heat transfer of the metal to the mold. Owing to the iron's temperature-dependent thermo-physical properties, this type of problem is of nonlinear characteristic. The results of the heat transfer are shown in 2D, as well as, the thermal flux, the thermal gradient and the convergence curves that control the feasibility of the Newton-Raphson algorithm calculation process. The cooling curves at various points of the solidified specimen, and the heating and cooling curves in the mold were also shown. These results were considered relevant.

***Keywords**:Numerical simulation, finite elements, solidification of iron, sand and mullite mold*

Introduction

The technological difficulties involved in casting processes vary considerably according to the metal's melting temperature characteristics, which in turn are related to the physicochemical properties and structures of metals and alloys. These difficulties also involve a series of properties, which include differences in chemical activities between the elements that constitute the alloy, solubility of the gases, method of solidification among the chemical elements, type of molding, and coefficients of solidification shrinkage. On the other hand, the cooling process also affects the flow of cast metal, influencing the mold filling and stability, allowing the occurrence of cooling stresses and properties changes in the final product, and producing variations in the geometrical dimensions, the shape of the surface finish and the quality of the cast part.

Some of the properties and characteristics most directly associated with the casting process are as follows, given by " Campbell (1991)":

Fluidity: the capacity to fill the mold, i.e., the ability of the cast metal to flow through the feed heads and passages and filling all the interstices of the mold. The main variables that affect the fluidity of the metal and that are inherent to the metal itself are the temperature, chemical composition, surface tension, superficial oxide films, the viscosity of the cast metal, the metallostatic pressure, as well as the thermal diffusivity of the mold, its hot tops, feeders and mold permeability.

Gases in cast metals: gases may be present in castings, in solution or in cavities (bubbles), or due to the formation of chemical compounds. Gases are usually associated with defects, which lead to production losses. Some of the problems resulting from the presence of gases are oxidation of the cast metal, differences in the solubility of gas in the solid and the cast metal, the formation of non-oxide compounds and of solid oxide films. Defects caused by the presence of gases in cast metal can be avoided by controlling the raw material and the environment, and by means of treatments and additives aimed at preventing the formation of gases.

Solidification of metals, studied by "Campbell (1991), Pariona et al. (2000), Flemings (1974)": solidification takes place through nucleation and growth of the solid phase under favorable thermal conditions. Homogeneous nucleation, which involves the formation and survival of solid nuclei whose radii are larger or equal to the critical radius, it depend of the free energy, volume and surface. Nucleation takes place below the melting temperature in equilibrium, characterizing the occurrence of thermal super-cooling. Heterogeneous nucleation, which is associated to the existence of substrates with characteristics physical-chemistries different of the element or alloy metallic in question, this nucleation type requires a significantly lower thermal super-cooling compared with the homogeneous nucleation, was studied by "Pariona et al. (2000)". From a practical standpoint, casting almost always occurs with heterogeneous nucleation, either on the walls of the mold or due to the presence of diverse elements in the bath. Nucleation is followed by growth of the solid phase, whose development depends on the thermal conditions during solidification and on the alloy composition. When the temperature is reduced uniformly throughout the liquid, extensive random nucleation occurs throughout the liquid. However, the practical conditions of heat flow promote the formation of temperature gradients in the liquid, which induce initial nucleation on the mold's walls, with grain growth taking place toward the center of the cast part. Nucleated grains with the most favorable orientation grow preferentially, advancing toward the bulk of the casting by progressive deposition of atoms in the solid-liquid interphase. Lateral growth is restricted by competitive growth, resulting in the formation of column-like and elongated grains growing in the direction of the thermal flow.

The present study investigated the solidification of pure iron in industrial greensand molds, AI 50/60 AFS, and mullite molds (the latter material is frequently used in the Shaw process). The thermo-physical properties were considered as a function of the temperature, i.e., thermal conductivity and enthalpy. The properties of the sand

Paper accepted July, 2005. Technical Editor: Atila P. Silva Freire.

and mullite were considered constant. The presence of the convection phenomenon on the external surface of the mold was also taken into account. This type of problem has a nonlinear characteristic and was solved by means of the finite element method and, to render the solution feasible, the convergence was controlled.

The purpose of this work was to make a comparative study of these different types of molds. As a result, heat transfer was observed in the cast metal, at the interface and in the mold, as well as cooling curves and local solidification at different points in the cast metal, beside, heat flux, thermal gradient, and heating and cooling curves at different points in the mold. Thus, the microstructural quality and mechanical properties of the cast part depend not only on the casting technique employed, but also on the characteristics and properties of the molding process and of the type of metal or alloy used in the casting.

Mold and Core Materials

The molds used in the casting can be of the collapsible type, it should be fragmenting after of each process concluded, or permanent type molds is used in the manufacture of large-scale of production.

The most common and low-cost collapsible molds are made of refractory materials based on silica sand. These molds are used in the industrial production of castings, serving for small, medium or large-scale production.

Permanent molds are usually made of steel or steel alloys and are used in the casting of metals or alloys with a lower melting point than the matrix, although other materials such as graphite may also be used. Due to the high manufacturing cost of permanent metallic molds or matrixes, they are applied only in large-scale industrial production.

Generally speaking, the type of mold employed strongly influences the quality of the cast part in terms of dimensions, shape, surface finish and internal quality; hence, it is indispensable the appropriate selection and control of the materials of which the mold is made, showed by "Campbell (1991)".

It is also worth noting that the material of the mold plays an important role in the casting's solidification. Because solidification is essentially the result of heat transfer during the process, the thermal properties of the mold material, such as thermal conductivity and diffusivity, affect not only the structure of the solidified part but also its properties and qualities, besides influencing the total solidification time and the cost of the productive process.

Numerical Simulation

Solidification/melting is accompanied by the release/absorption of latent heat at the solid-liquid and solid-solid interfaces. Consequently, solidification process involves phase changes, in this case, the enthalpy method is the modeling more appropriate to describe this process, because, in this method the latent heat is inserted that represents the phase transformation. Then, the general differential equation of heat conduction for the transient nonlinear state that describes this phenomenon were presented by "Su (2001)", "Shi and Guo (2004)", "Radovic and Lalovic (2005)", "Janik and Dyja (2004)":

$$K\left(\frac{\partial^2 T}{\partial x^2}+\frac{\partial^2 T}{\partial y^2}+\frac{\partial^2 T}{\partial z^2}\right)=\frac{dh}{dt} \quad (1)$$

Where the enthalpy, $h=\int \rho c dT$

The heat transfer mechanism by convection is established as the boundary condition:

$$q = K\frac{\partial T}{\partial x}\bigg|_{x=0} = K\frac{\partial T}{\partial y}\bigg|_{y=0} = K\frac{\partial T}{\partial z}\bigg|_{x=0} = h_f\left(T - T_{ambiente}\right) \quad (2)$$

where q is the heat, K is the thermal conductivity, c is the specific heat, and ρ is the density of the material. These properties may be temperature-dependent then Equation (1) is transformed into a nonlinear transient equation. h_f is the coefficient of convective heat transfer on the mold's external surface, T is the temperature, and T_B is the temperature of the environment.

Through Equations (1) and (2) one can determine the distribution of temperature or transfer of heat during the process of solidification in the casting of pure iron in sand or mullite molds.

Convergence Criteria

A nonlinear thermal solution typically requires that special loading and controls be activated in Ansys software. Specifically, it can be needed to divide loads into smaller increments to insure convergence, control convergence criteria, invoke convergence enhancement tools, control program behavior in the event of non-convergence and manage the large volume of information that is typically generated during a nonlinear analysis. A brief review of the basic concepts of the criterion of convergence control is given below. Further details are available in the Thermal Analysis Guide "Handbook Ansys 9.0, 2005".

If one defines $\{Q^a\}$ as the vector of internal nodal heat flow arising from the computed calculation, $\{Q^{nr}\}$ as the vector of nodal heat flow from its application, and $\{\Phi\}$ as the out-of-balance heat flow vector or "residual" as the difference between the two vectors, then second "Ansys (2005)",

$$\{\Phi\} = \{Q^a\} - \{Q^{nr}\} \quad (3)$$

Also defining the norm (i.e., magnitude) of the residual, represented by $\|\Phi\|$. A convergence criterion is usually equal to the norm of the applied load vector, $\|Q^a\|$, multiplied by a small tolerance factor, ε.

The governing equation for thermal analysis of a nonlinear system is written in matrix form as, "proposed by Ansys (2005)":

$$[h(T)]\{\dot{T}\} + [K(T)]\{T\} = \{Q(T,t)\} \quad (4)$$

where [h(T)] is the enthalpy matrix, [K(T)] is the conductivity matrix and {Q(T,t)} is the heat flow term.

For a single-field nonlinear thermal analysis, ANSYS will always use the full Newton-Raphson iterative algorithm. This technique follows the process below:

1. The incremental form of the system equations is solved, second "Ansys (2005)"

$$[h(T_{i+1})]\{\dot{T}_{i+1}\} + [K(T_{i+1})]\{T_i + 1\} = \{Q^a\} - \{Q^{nr}_{i+1}\},$$
$$(i = 1, 2, \ldots\ldots), \text{ where } \{T_{i+1}\} = \{T_i\} + \{\Delta T_i\}$$

2. The nodal temperature is updated,
3. Internal nodal heat flow rates are calculated from elemental heat fluxes,

4. The convergence norm is computed and compared against the criterion:

If the norm is equal to or lower than $\|\{\Phi\}\| \le \varepsilon \|Q^a\|$, no further iterations are performed.

If the norm is higher than $\|\{\Phi\}\| > \varepsilon \|Q^a\|$, $[K^T]$ is updated and another iteration is performed and the default value for ε is 0.001. Since nonlinear analyses typically require incremental loading to obtain converged solutions, Substeps are used to differentiate intermediate converged solutions within a Load Step.

Considering some nomenclatures and condition for the convergence criterion supplied by the software, where, the Graphical Solution Tracking (GST) monitor plots the "Absolute Convergence Norm" ($\|\Phi\|$), denoted for "Heat L2", and the criteria ($\varepsilon \|Q^a\|$), denoted for "Heatcrit", both are represented as a function of the "Cumulative Iteration Number". The convergence of the solution is reached when "Heat L2" is smaller or equal that the criterion "Heatcrit".

Methodology of the Numerical Simulation

Ansys software programs were used to simulate the solidification of pure iron in green-sand and mullite molds, with the aid of a Pentium III 1GHz microcomputer. The following procedures were adopted for the simulations:

a) Geometrical design of the part: For this purpose, a corner piece of pure iron was used, a material with homogeneous and isotropic characteristics, as illustrated in Figure 1.

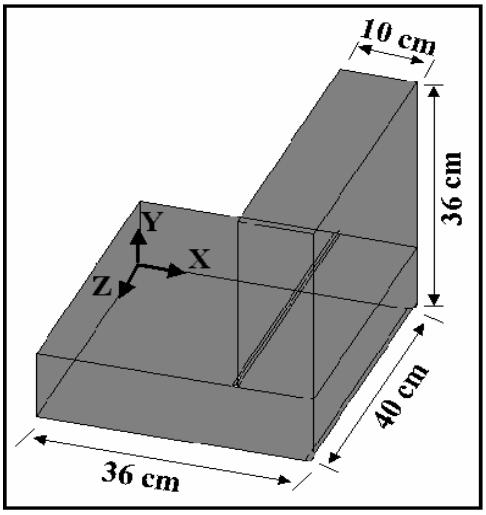

Figure 1. Corner piece of iron.

b) The geometry of the cast part was designed together with the greensand or mullite mold. This geometry is illustrated in Figure 2 (a), which represents the symmetry in three-dimensions, showing the entry of the cast metal in the upper part of the figure. The simulation did not consider the positioning of the feed head, hot top and conventional mold model was used. The symmetry was used in order to reduce the number of grid points, i.e., to facilitate the computation of the system of nonlinear equations and avoid overloading the computer's capacity. However, in this work the analysis was made for half symmetry in 2-D, which is illustrated in Figure 2 (b). The mesh was more concentrated in the cast metal that in the mold, because the most interesting phenomena happen inside of the cast metal, being the mesh size in the mold was of 0.45 cm and in the cast metal it was of 0.2 cm.

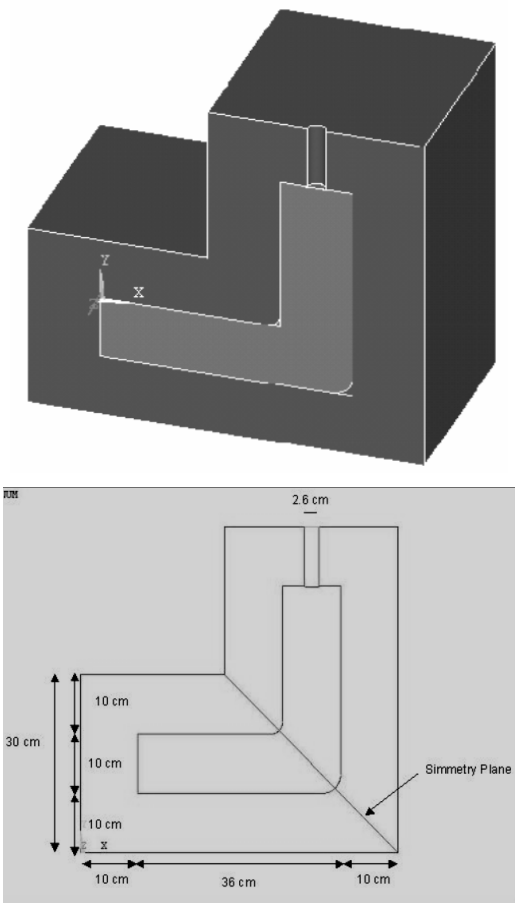

Figure 2. Symmetry of the cast part and mold in 3-D and 2-D.

c) The materials used in this work were pure iron and sand or mullite, and their properties are shown in Table 1.

The phase transformation of pure iron may be represented as follows, "Upadhyaya and Dube (1977)":

$$< \alpha, Fe > \overset{1033K}{\rightarrow} < \beta, Fe > \overset{1183K}{\rightarrow} < \gamma, Fe > \overset{1673K}{\rightarrow} < \delta, Fe > \overset{1812K}{\rightarrow} \{Fe\} \quad (5)$$

The properties, such as, specific heat (C_P) and latent heat (ΔH) are shown for pure iron in function of the temperature (T). They are shown as follow:

$C_{P,<\alpha\text{-}Fe>} = 17.49+24.77x10^{-3}T$ J/K.mol, $C_{P,<\beta\text{-}Fe>} = 37.66$ J/K.mol,
$C_{P,<\gamma\text{-}Fe>} = 7.70+19.50x10^{-3}T$ J/K.mol, $C_{P,<\delta\text{-}Fe>} = 43.93$ J/K.mol,
$C_{P,\{Fe\}} = 41.84$ J/K.mol, $<\alpha\text{-}Fe> \rightarrow <\beta\text{-}fe>$;

$\Delta H^o_{1033} = 2761.4\,J/mol$, $<\beta\text{-}Fe> \rightarrow <\gamma\text{-}Fe>$;

$\Delta H^o_{1673} = 690.4\,J/mol$, $<\gamma\text{-}Fe> \rightarrow <\delta\text{-}Fe>$; $\Delta H^o_{1673} = 690.4\,J/mol$

and $<\delta\text{-}Fe> \rightarrow \{Fe\}$; $\Delta H^o_{1812} = 15{,}355\,J/mol$. (6)

Density of pure iron =7870 Kg/mol and atomic weight = 56.0.

Through these data, the enthalpy was calculated for pure iron, as shown in Table 1.

Table 1. Physical properties of the steel, the industrial sand, AI 50/60 AFS, and mullite, according to "Kingery et al. (1976), Hertzberg (1996), Ozisik (1985)".

Properties of the pure iron			
Temperature (K)	Enthalpy (MJ/m^3)	Temperature (K)	Thermal conductivity ($W.m^{-1}.K^{-1}$)
298	0	273	59.5
373	200.75	373	57.8
473	498.87	473	53.2
573	831.83	746	49.4
673	1199.61	673	45.6
773	1602.22	773	41.0
873	2039.65	873	36.8
973	2511.91	973	33.1
1033	3200.23	1073	28.1
1073	3412.0	1273	27.6
1183	4120.86	1473	29.7
1273	4453.89		
1373	4849.96		
1473	5273.45		
1573	5724.36		
1673	6299.75		
1812	9317.24		
1812	9676.0		
Density ($kg.m^{-3}$)	7870		
Melt temperature 1812 K			
Properties of the industrial sand, AI 50/60 AFS			
Specific heat			1172.3 $J/(kg.K)$
Thermal conductivity			0.52 $W/(m.K)$
Density			1494.71 kg/m^3
Properties of mullite			
Specific heat			1172.3 $J/(kg.K)$
Thermal conductivity			5.86 $W/(m.K)$
Density			3100 kg/m^3
Convection properties			
h_f, coefficient of convective heat transfer on the external surface of the mold			11.45 $W/m^2.K$
T_B, temperature of the environment			300 K
Initial temperature of the liquid metal (super-heating in 111 K)			1923 K

Thermal conductivity for pure iron was approximate, according with the data of AISI-SAE 1008 steel, "Metal Handbook, v.1 (1978)".

d) In order to generate the system of equations, as well as to find the result at each point of the cast part, a mesh was generated throughout the area of each part. The geometrical unit of each mesh element must fit the geometry of the part. In order to achieve this, the ANSYS program allows for control of the size and geometry of the mesh in order to obtain the most precise solution. However, a very large number of grid points can compromise the computer's capacity. Figure 3 shows the mesh element and the mesh in the symmetry of the part, according to "Handbook Ansys 9 (2005)".

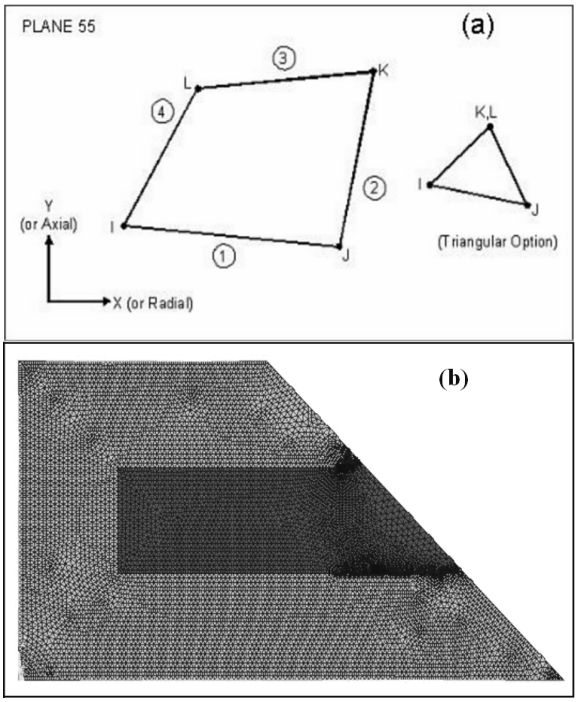

Figure 3. (a) Type of mesh element used for the simulation of heat transfer (b) the mesh in the part's symmetry.

e) The initial and boundary conditions were then applied to the symmetry of the parts. The initial conditions for the mold was the environmental temperature (300 K) applied on the outside wall of mold, and the cast metal temperature was considered as 1923 K, since the melting temperature of this type of metal is 1812 K; in other words, the cast metal was superheated in 111 K. The boundary condition was the convection phenomenon generated by the natural aerated environment. This phenomenon was applied on the outside wall of mold. This phenomenon is represented by Equation (2) and the coefficient of convective heat transfer is shown in Table 1. The effects of the application of refractory paint and of the gassaging process were not taken into consideration either.

f) The final step consists in solving the problem of heat transfer of the mold – cast metal system, using Equations (1) and controlled by the convergence condition. The time of processing for the simulation was of 3 hours. The result of the heat transfer is shown in 2-D, as well as the heat flux, the thermal gradient, the cooling curves in different points in the cast metal, and the heating and cooling curves in the different points in the mold.

Results and Discussion

In this study, an analysis of heat transfer for the casting process in two dimensions was made for the nonlinear case. The idea was to determine the distribution of temperature, heat flux, thermal gradient, cooling curves in the cast metal, and heating or/and cooling in the molds during casting process of pure iron in greensand and mullite molds during 1.5 hours of solidification. The phenomenon of convection that occurs between the mold and the environment was included in this study. In this case, the properties

of the mold materials were considered as constant. However, enthalpy and thermo-physical property of pure iron was considered as a function of the temperature. The effect of radiation was ignored here.

The numerical simulation of solidification using the Ansys 9 software program was performed for a pure iron corner piece in an industrial greensand mold, AI 50/60, dry, and in a mullite mold as illustrated in Figure 4. This figure shows the results after 1.5 hours of solidification, for which the increment of each substep of time was 5 seconds. However, the melting temperature of pure iron is 1812 K and, in this study, the cast iron was superheated to 111K above the melting temperature in order to observe the heat transfer above that temperature.

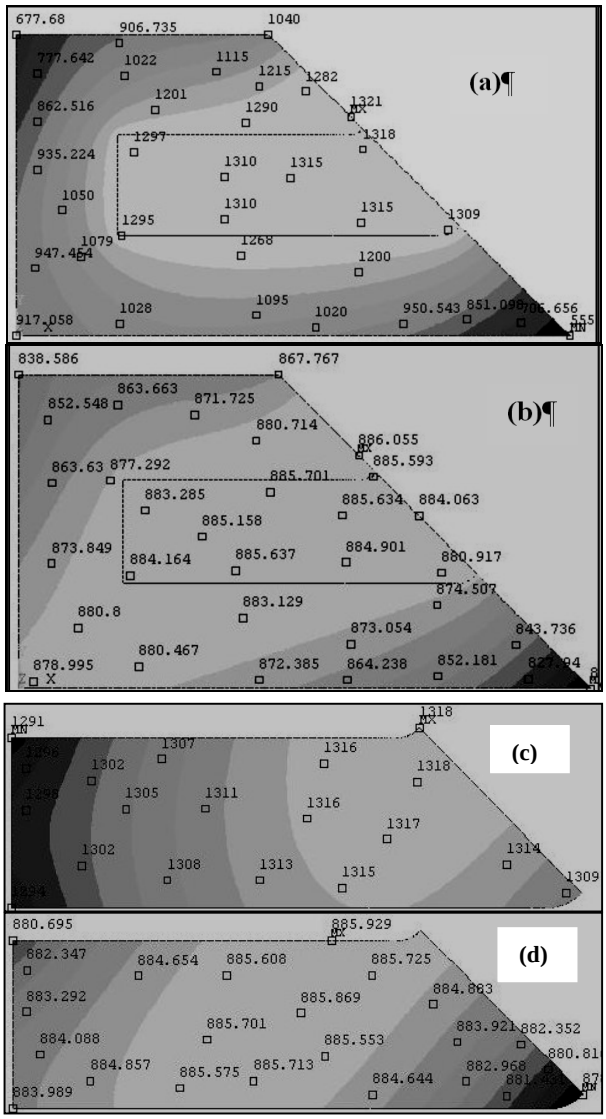

Figure 4. Temperature distribution in the (a) sand mold system, (b) mullite mold system, (c) inside of the cast metal in sand mold and (d) inside of the cast metal in mullite mold.

In Figure 4, the distributions of the temperatures can be observed in whole system in both molds, as well as in the cast metal (where the numbers inside the graphs represent temperatures in degrees K), after a 1.5 hours of solidification. The results showed a difference in the temperature distribution in both systems. Comparing graphs (a) and (b), the sand mold had a range of temperature variation between 555 and 1321 K and the mullite mold had a range of 803 and 886 K, consequently, in the sand mold there was a larger range of temperature variation. Observing the cast metal, shown in graphs (c) and (d) in more detail, it is also noticeable that a larger range of temperature variation happened inside the sand mold. That is because the physical properties of the molds are different. It is also noticeable, that the maximum points (MX) of temperature for both cast metals are located in points a little displaced from one another, and that the minimum points (MN) are located in different positions, although these points should be located in the same position as in graph (c). This point (MN) in graph (d) suffered a displacement; this could be due to some type of minimum numeric mistake, as can be observed in the graphs.

In Figure 5, the result of the thermal flow is presented for both systems, in magnitude, shown in graphs (a) and (b), as well as in vectorial form, in graphs (c) and (d). Through these graphs it can be observed that a larger thermal flow happened in the sand mold than in the mullite mold. In both systems it is noticeable that the maximum point (MX) of thermal flow is located at the same point, however, the minimum (MN) of the thermal flow is a little dislocated. In this figure it can be observed that the largest magnitude of the thermal flow corresponds to the minimum point (MN) of the temperature distribution (Fig. 4), because at this point the solidification begins. Besides, in graphs (c) and (d) of Figure 5, the vectors indicate the largest variation of thermal flow; this could be due to a lesser thickness of the mold influenced by the convection phenomenon.

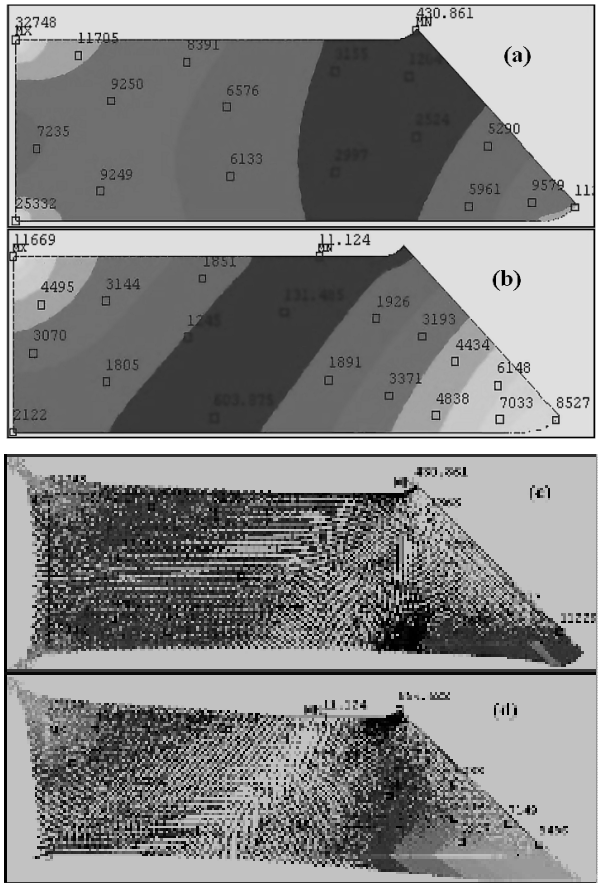

Figure 5. Heat flux (W/m2) in magnitude (a) inside of the cast metal with sand mold (b) inside of the cast metal with mullite mold and in vectorial form (c) inside of the cast metal with sand mold (d) inside of the cast metal with mullite mold.

In addition, the thermal gradients were determined for both systems. The result is presented in Figure 6, in magnitude and in the vectorial form. As can be seen in the graph, the thermal gradient is larger in the sand mold than in the mullite mold. Also, the maximum and minimum thermal gradients are exactly located in the same points where they happened in the thermal flow. In this case, it is noticeable in graphs (c) and (d), that the direction of the thermal gradient is contrary to the thermal flow. The direction of the thermal gradient corresponds to the direction of the solidification, from the cold zone to the hot zone.

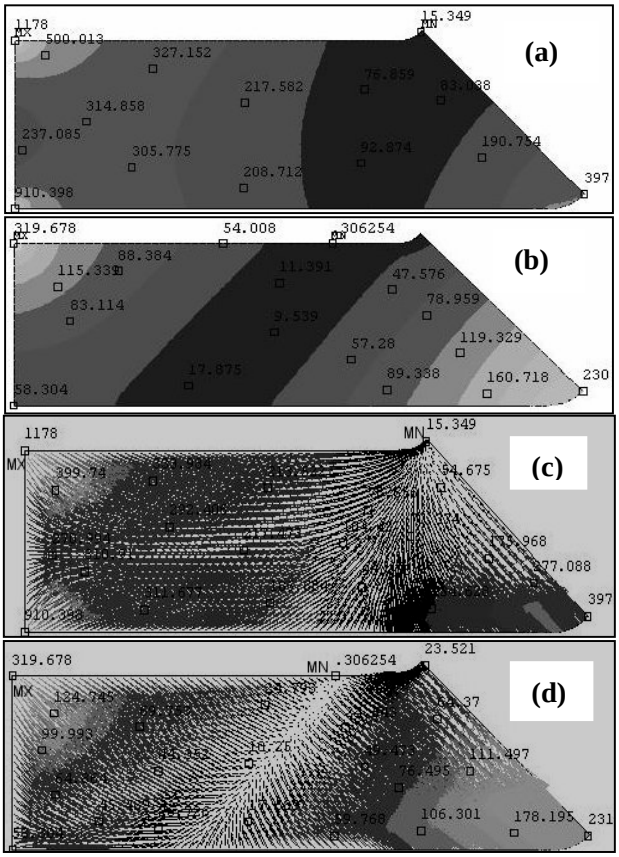

Figure 6. Thermal gradient (k/m) in magnitude (a) inside of the cast metal with sand mold (b) inside of the cast metal with mullite mold and in vectorial form (c) inside of the cast metal with sand mold (d) inside of the cast metal with mullite mold.

The convergence of the simulation process was verified in Figure 7, because the literature examined establishes that Heat L2 should be smaller than or equal to Heatcrit in order to reach the convergence of the nonlinear system. In these graphs it can observed that the number of iterations necessary to reach the convergence is larger for the mullite mold than for the sand mold, and in both systems the solidification time was fixed in 1.5 hours.

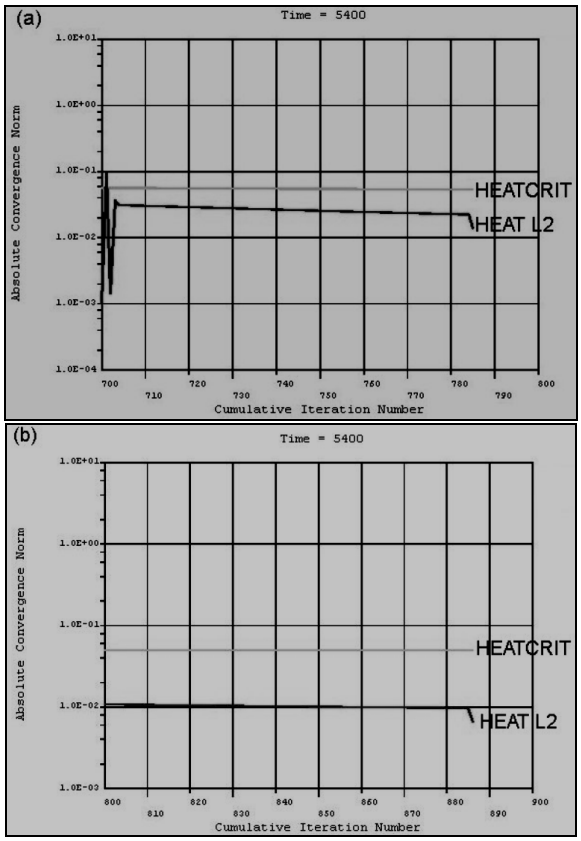

Figure 7. Result of the convergence of model for the solidification of iron in sand and in mullite molds.

In this work, such as, the solidification process in the cast metal and the processes of heating and cooling in the molds were also studied. The variation of temperature in function of the distance for different paths selected in the cast metal system and in the mold were also studied. For this purpose, Figure 8 was considered.

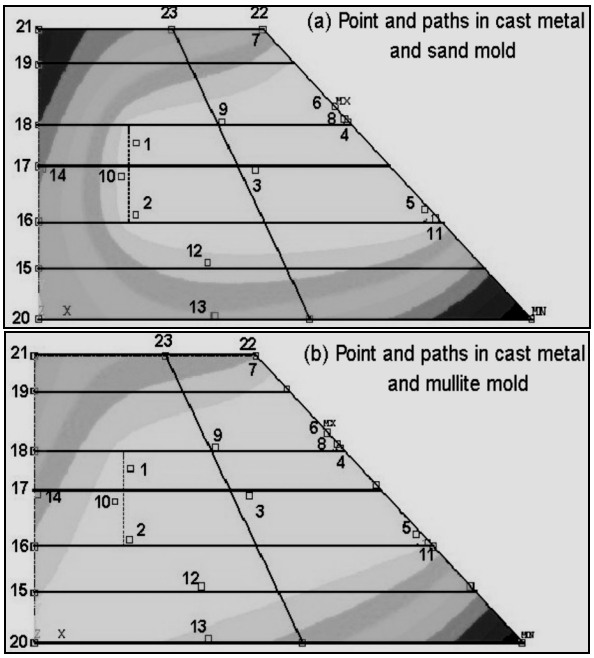

Figure 8. Points and paths in the sand and mullite systems.

In Figure 8, for both systems the same points were selected inside the cast metal (1, 2, 3, 4 and 5), in order to study the solidification process, and the points inside the mold (6, 7, 8, 9, 10, 11, 12, 13 and 14), in order to study the heating and/or cooling process. Inside the cast metal that corresponds to the sand mold, the cooling curves for the solidification process are shown in Figure 9 (a). At points 3 and 4, the phase changes are observed at the temperatures of 1816 K (from liquid iron to iron δ) and at 1671 K (from iron δ to iron γ), this last transformation also happens for point 5. These phases transformations can be verified in Equation 5 as well as in Table 1. The phase changes were observed at the points where the cooling is slower. When the cooling is fast, it is not possible to observe the curvatures of phase change. Possibly, the phase transformation is controlled by the diffusion phenomenon. When the cooling velocity is slow, the curvature of phase change can be observed.

In Figure 9 (b) the cooling curves inside the cast metal that corresponds to the mullite mold is presented. At points 3, 4 and 5 the phase transformation at 1070 K was observed, and at points 1 and 2 the phase transformation at 974 K was seen. The phase transformations at points 1, 2, 3, 4 and 5 are possibly from iron β to iron α, which can be verified approximately by Equation 5 and Table 1. This type of dislocation of the phase transformation can be due to the phenomenon of super-cooling [3], convection phenomenon that influences the cooling velocity [4, 13, 14, 15]. Consequently, the phase transformation behavior that happens in cast metal inside of the mullite mold is totally different form that which happens in the sand mold.

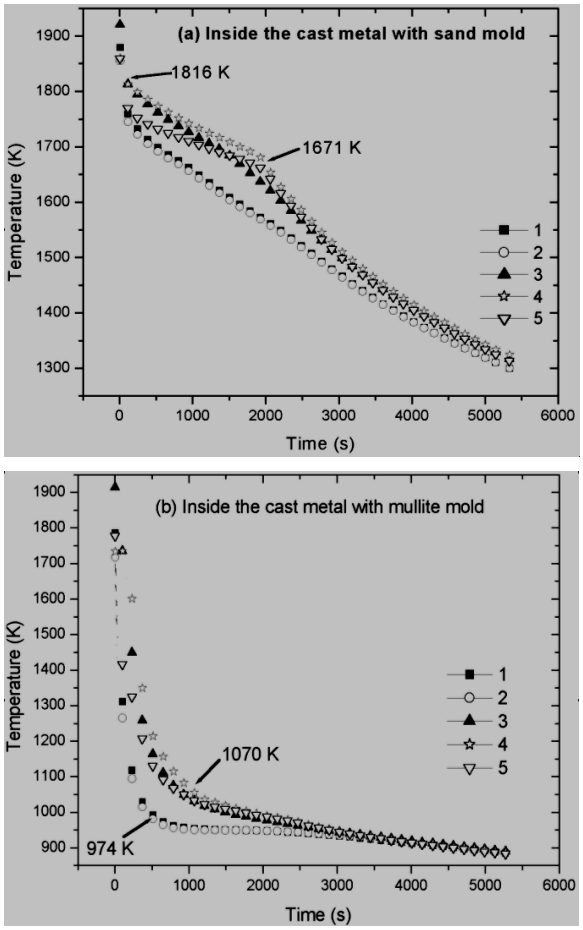

Figure 9. Cooling Curves of cast metal in sand and in mullite molds.

The heating and cooling curves are presented in the curves (a) of Figure 10, for the sand mold, where points 6, 8, 9, 10 and 11 present the heating and cooling behavior, because these points are near the cast metal. However, at points 7, 12, 13, and 14 only the heating behavior can be observed, because these points are far from the cast metal. In Figure 10 (b) the heating and cooling curves in the mullite mold are presented at points 6, 8, 9, 10 and 11 there is an abrupt heating, and cooling presents an accentuated fall, as compared with the sand mold. On the other hand, at points 7, 12, 13 and 14 only the cooling curves are presented, because they are far from the cast metal. As can be observed in both systems, all the cooling curves tend to converge, and this convergence is faster for the mullite mold.

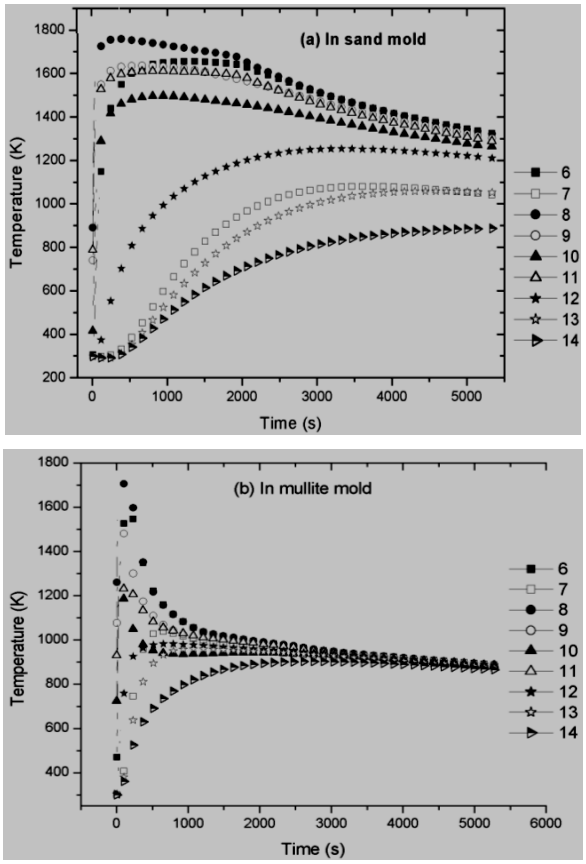

Figure 10. Cooling and/or heating curves in sand and in mullite molds.

The behavior of temperatures in different paths selected in the sand and mullite systems was also studied, as shown in Figure 8. The result can be observed in Figure 11. As can be seen in both systems, in paths 16, 17, 18, 22 and 23 there is an accentuated plateau, because these paths go through the cast metal. This plateau is higher in the sand system than in the mullite system because cooling is slower in the sand system. Also, in the path 15 there is a high plateau in both systems, because this path is out the cast metal, although it crosses a fairly hot zone. On the other hand, paths 19, 20 and 21 are far from the cast metal, and in these cases heating and cooling can occur, except in path 21 in which heating only occurs.

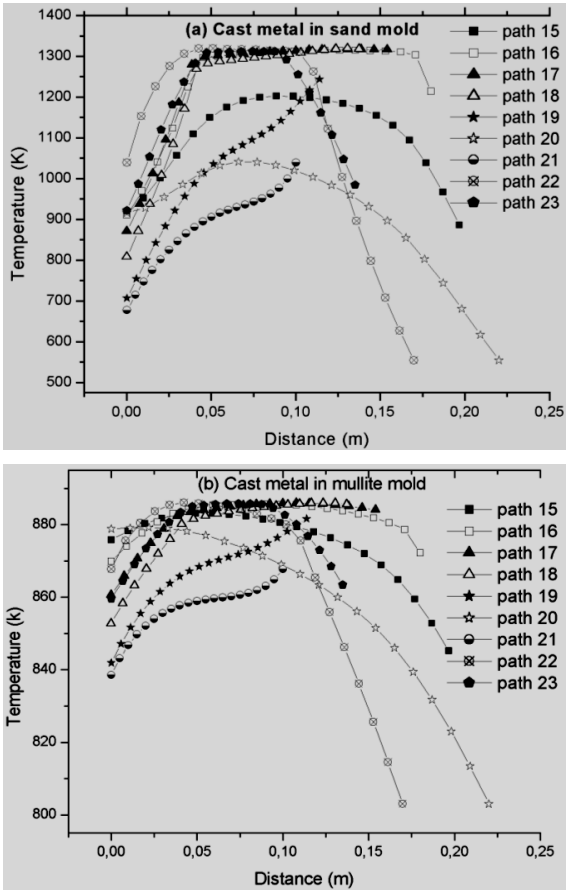

Figure 11. Behavior of temperature in different paths in the sand and mullite systems.

Conclusions

This study is a comparative work of the numeric simulation by the finite element method of the solidification process of pure iron in sand and in mullite molds, during 1.5 h of solidification. Results in 2D were obtained, such as the heat transfer, the thermal flow, the thermal gradient, the convergence control and the behavior of the temperature in different selected paths. The result was completely different in both systems. This can be due to the fact that these molds possess different physical properties. Therefore, cooling in the sand system was slower than in the mullite system. This fact caused a larger thermal flow and thermal gradient in the sand system than in the mullite system. These phenomena happen especially in the cold zone of the cast metal, where the solidification begins. It was also observed that, in the convergence process, the mullite system needed a larger iteration number, probably because it reached lower temperatures than the sand system, during the same time of solidification. In the cooling curves, at several points of the sand system presented phase changes, however, this did not happen in the mullite system. This phenomenon can be explained by the fact that in the sand system the cooling is slower than in the mullite system. Possibly in the sand system the diffusion phenomenon prevails. The cooling curves characterize the grain size and mechanical properties of metal; hence, owing to the smaller grain size of metal cast in mullite molds, this type of mold grants better mechanical properties to the cast part. The cooling and/or heating in the molds was also studied, and in the mullite mold the heating and cooling are abrupt, but all the curves in both systems tend to converge.

References

[1] Campbell, J., 1991, "Casting", Butterworth-Heinemann, Oxford.

[2] Pariona, M.M., Bolfarini, C., dos Santos, R.J. and Kiminami, C.S., 2000, "Application of Mathematical Simulation and Factorial Design Method to the Optimization the Atomization Stage in the Forming of a Cu-6% Zn Alloy", Journal of Materials Processing Technology, v.102, n.1, pp. 221-229.

[3] Flemings, M.C., 1974, "Solidification processing", McGraw-Hill, New York.

[4] Su, X.., 2001, "Computer aided optimization of an investment bi-metal casting process", Ph.D. Thesis, University of Cincinnati, Department of Mechanical, Industrial and Nuclear Engineering.

[5] ASM Hanbook, 1996, "Casting" v.15, The materials Information Society.

[6] Ansys, 2005, "Heat Transfer 9 Training-Manual", Ansys, Inc., Canonsburg, PA.

[7] Grozdanic´, V., 2002, "Numerical simulation of the solidification of a steel rail-wheel casting and the optimum dimension of the riser" , Materiali in tehnologije, v. 36, pp.39-41.

[7] Davies, A. J., 1980, "The finite element method", Oxford University Press, New York.

[8] Handbook Ansys 9, 2005, Ansys, Inc., Canonsburg, PA.

[9] Upadhyaya, G.S., Dube, R.K., 1977, "Problems in metallurgical thermodynamics and kinetics", Pergamon Press, Oxford.

[10] Metal handbook, ninth ed., v.1, 1978. "Properties and selection: iron and steel", American Society for Metals, Oshio.

[10] Kingery, W. D.; Bowen and H. K.; Uhlmann, H. K., 1976, "Introduction to ceramics", 2nd ed., John Wiley, New York.

[11] Hertzberg, R.W., 1996, "Deformation and fracture mechanics of engineering materials", John Wiley & Sons, New York.

[12] Ozisik, M.N., 1985, "Heat Transfer a basic Approach", McGraw-Hill, New York.

[13] Shi, Z, Guo, Z.X., 2004, Numerical heat transfer modelling for wire casting, Materials Science and Engineering, v.A365, p. 311–317.

[14] Radovic, Z., Lalovic, M., 2005, Numerical simulation of steel ingot solidification process, Journal of Materials Processing Technology, v.160, p.156–159.

[15] Janik, M., Dyja, H. , 2004, Modelling of three-dimensional temperature field inside the mould during continuous casting of steel. Journal of Materials Processing Technology, v. 157–158, p. 177–182.